Available online at www.sciencedirect.com

SciVerse ScienceDirect

Procedia Computer Science 9 (2012) 699 – 706

Procedia Computer Science

International Conference on Computational Science, ICCS 2012

Slope stability assessment using stochastic rainfall simulation

Joshua A. White[1]

Computational Geosciences Group, Lawrence Livermore National Laboratory

Dashi I. Singham

Operations Research Department, Naval Postgraduate School

Abstract

Many regions around the world are vulnerable to rainfall-induced landslides and debris flows. A variety of methods, from simple analytical approximations to sophisticated numerical methods, have been proposed over the years for capturing the relevant physics leading to landslide initiation. A key shortcoming of current hazard analysis techniques, however, is that they typically rely on a single historical rainfall record as input to the hydromechanical analysis. Unfortunately, the use of a single record ignores the inherently stochastic nature of the rainfall process. In this work, we employ a Markov chain model to generate many realizations of rainfall time series given a measured historical record. We then use these simulated realizations to drive several hundred finite element simulations of subsurface infiltration and collapse. The resulting slope-stability analysis provides an opportunity to assess the inherent distribution of failure statistics, and provides a much more complete picture of slope behavior.

Keywords: Slope-stability, rainfall, unsaturated flow, Markov process, finite element method

1. Introduction

Rainfall induced landslides and debris flows cause thousands of deaths and severe infrastructure damage each year. The ability to model and forecast landslide hazards is therefore of crucial interest in vulnerable regions around the world. In many cases, landslides on steep soil slopes are triggered by heavy rainfall infiltrating into the subsurface. Increasing fluid saturation leads to a loss of capillary suction and an increase in soil unit weight, two processes which tend to destabilize the slope. This hydromechanical behavior may be readily modeled using a variety of methods, from simple analytical approximations to sophisticated numerical methods. Most of these analyses, however, are deterministic in nature and ignore the uncertainty associated with future rainfall patterns. The current paper is motivated by this crucial shortcoming.

Over the years, a variety of models for slope hazard assessment have been proposed. These models can be roughly classified into two broad categories: (1) site-specific models and (2) regional models. The essential difference between the two is the level of site characterization data that is available. If sufficient information about the local topography,

Email addresses: jawhite@llnl.gov (Joshua A. White), dsingham@nps.edu (Dashi I. Singham)

[1]Corresponding author

doi:10.1016/j.procs.2012.04.075

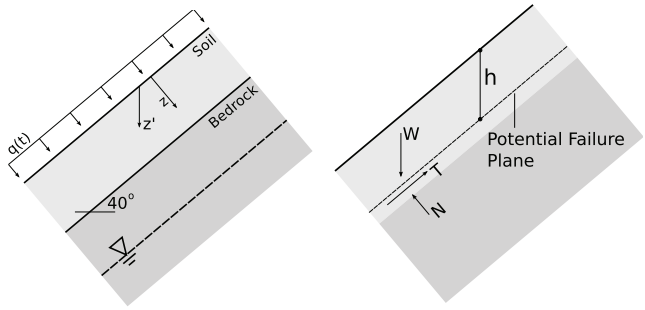

(a) Infiltration problem (b) Limit-equilibrium problem

Figure 1: Geometric configuration of the slope stability problem, illustrating both hydrologic and mechanical parts.

stratigraphy, soil constitutive properties, and water table conditions are available, a full-physics model can be justified for examining the failure potential at a given site. See, for example, the hydrologic model discussed in [1] and coupled hydromechanical models in [2, 3]. However, a preliminary hazard assessment is often required at a regional level to identify high-risk areas. At this scale, only the crudest characterization data is available. This is often not much more than a digital elevation map and a rough estimate of "typical" soil properties in the region. In these situations, simple numerical or empirical models are often adopted, as there is insufficient data to constrain anything more sophisticated. See, for example, [4, 5].

In either case, a necessary input to the models is the rainfall record $q(t)$ that drives the slope failure process. A key shortcoming of current hazard assessments, however, is that they typically rely on a single historical rainfall record. The use of a single record ignores the inherently stochastic nature of the rainfall process, and provides an incomplete picture of slope behavior. In this work, we employ a Markov chain model to generate many realizations of rainfall time series given a measured historical record. We then use these simulated realizations to drive several hundred finite element simulations of subsurface infiltration and collapse. The resulting slope-stability analysis provides an opportunity to assess the inherent distribution of failure statistics, including the cumulative infiltration at failure and the time to failure.

For clarity of exposition, in this work we adopt a highly-simplified "infinite-slope" approximation for slope behavior, an approach that is often applied at the regional level. We remark, however, that the proposed methodology may just as easily be applied to more sophisticated numerical models of slope behavior. This is the subject of ongoing work. We also note that we ignore several other sources of uncertainty, such as material properties or geometric configuration. In practice these uncertainties are highly relevant as well, but they are epistemic in nature and may, in principle, be reduced with additional site characterization efforts. This should be contrasted with the aleatoric nature of future rainfall.

2. Slope failure model

Figure 1 illustrates the geometry under consideration, consisting of an inclined slope at angle $\alpha = 40°$ that extends infinitely in either direction. This approximation may reasonably be applied to an actual field site if the local curvature of the slope is small, and if the time-scale of interest for infiltration normal to the slope is much shorter than the time-scale for slope-parallel flow. The stratigraphy consists of a homogeneous soil layer 1 m deep which overlies a rigid and impermeable bedrock layer. The initial water table lies 2 m below the ground surface, so that the soil layer is initially unsaturated. As rainfall proceeds, water is assumed to infiltrate in a wetting front that propagates normal to the ground surface. The geometry and boundary conditions are such that both the infiltration and mechanical stability may be analyzed using one-dimensional approximations.

Prior to failure, it is reasonable to assume that mechanical deformations in the pore space are minor and may be

Table 1: Constitutive parameters for the slope-stability simulations.

Parameter	Symbol	Value	Units
Porosity	n	0.4	
Solid Density	ρ_s	2.0	Mg/m^3
Fluid Density	ρ_w	1.0	Mg/m^3
Intrinsic Permeability	k	10^{-11}	m^2
Dynamic Viscosity	η	10^{-6}	kPa·s
Residual Saturation	ψ_1	0.32	
Maximum Saturation	ψ_2	1.0	
Scaling Suction	s_a	2.0	kPa
Shape Parameter	n	1.5	
Shape Parameter	m	$(n-1)/n$	
Cohesion	c	0	kPa
Friction Angle	ϕ	35.0	deg.

ignored. Infiltration may then be adequately described by a one-dimensional version of Richards' equation,

$$n\frac{\partial \psi(p)}{\partial t} - \frac{\partial}{\partial z}\left[\frac{k k_r(\psi)}{\eta}\left(\frac{\partial p}{\partial z} + \rho_w g \cos\alpha\right)\right] = 0 \tag{1}$$

Here, n is the soil porosity, ψ is the water phase saturation, k is the intrinsic permeability, k_r is the relative permeability, η is the dynamic viscosity, p is the fluid pressure, and ρ_w is the fluid density. The model must be supplemented with constitutive models for the pressure/saturation relationship $\psi(p)$ and saturation/relative-permeability relationship $k_r(\psi)$. In this work, we adopt the van Genuchten/Mualem model [6]. The model also requires appropriate initial and boundary conditions. The weak form is then discretized using a Galerkin finite element scheme in space and a backward Euler scheme in time. Extensive details on the numerical implementation are provided in [7] and are omitted here for brevity.

Having solved for the pressure field $p(z,t)$, we may assess how close the slope is to failure at time t using a simple limit-equilibrium analysis. Due to the kinematics of the infinite slope approximation, when the slope fails it must fail along a plane parallel to the ground surface (Figure 1b). Due to the self-weight W of the overlying solid/fluid mixture and basic geometric considerations, the normal and tangential forces N and T acting on a plane at vertical depth h may be readily computed. The resulting normal and tangential stresses are given by

$$\sigma = \omega \cos^2\alpha \qquad \text{and} \qquad \tau = \omega \cos\alpha \sin\alpha \tag{2}$$

where

$$\omega = \int_0^h \rho g \, dz' = \int_0^h \left[(1-n)\rho_s + n\psi\rho_w\right] g \, dz' \tag{3}$$

is the self-weight of a unit column of soil above the failure plane. Note that this integration takes place over the vertical coordinate z' rather than the slope normal coordinate z. We then assume that the mobilized shear strength of the soil can be described by a Mohr-Coulomb model,

$$\overline{\tau} = c + \sigma' \tan\phi, \qquad \text{with} \qquad \sigma' = (\sigma - \psi p) \tag{4}$$

where c is the soil cohesion, ϕ is the friction angle, and σ' is the effective normal stress. Note that we have adopted a particular form here for the effective stress decomposition, using a saturation-weighted suction stress $\sigma_s = \psi p$. The slope will fail when the applied shear stress exceeds the mobilized shear strength, $\tau > \overline{\tau}$, at the current state $\{\sigma, p, \psi\}$. It is convenient then to define a factor-of-safety F representing the ratio of these two quantities,

$$F = \frac{\overline{\tau}}{\tau} = \frac{\tan\phi}{\tan\alpha} + \frac{c - \psi p \tan\phi}{\omega \cos\alpha \sin\alpha} \tag{5}$$

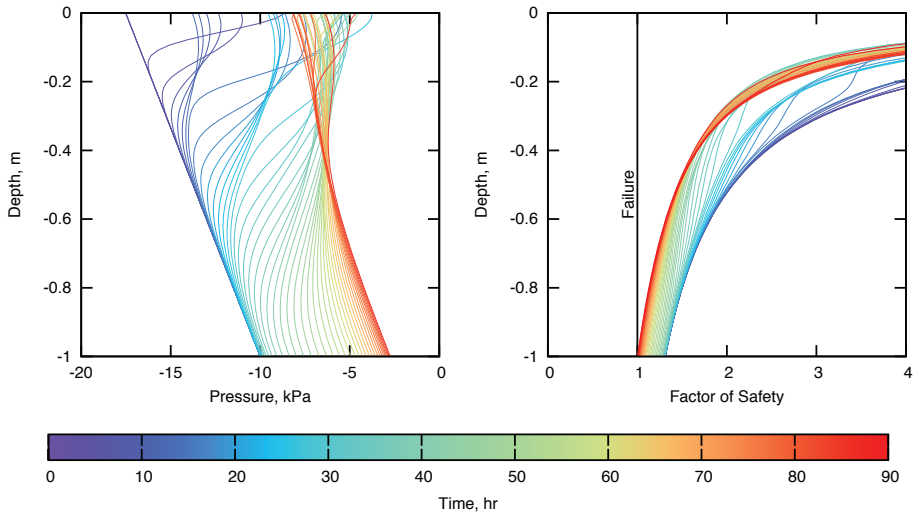

Figure 2: Time evolution of pressure (top) and factor of safety (bottom) over the soil depth, using a single rainfall realization.

with $F = 1$ denoting a state of limit equilibrium and $F < 1$ indicating failure. From this expression, it is apparent that slope stability derives from three components: a friction component, a cohesion component, and a suction stress component. While the cohesion and friction angle remain constant during the rainfall infiltration process, induced changes in the suction stress σ_s and soil weight ω may drive the slope to failure.

The constitutive parameters used for all simulations in this paper are presented in Table 1. Figure 2 plots results from a simulation using a typical input rainfall record. The water pressure in the slope begins in hydrostatic equilibrium, with a pressure gradient determined by the density of water and the slope angle. As rainfall proceeds, water infiltrates into the subsurface, leading to increasing pressure and saturation, and a decreasing factor of safety. While in principle the slope may fail at any depth within the soil layer, the minimum factor of safety for this example occurs at the soil/bedrock interface. When a factor of safety $F < 1$ is encountered, the slope is assumed to fail and the simulation ends. Various failure statistics such as time to failure and total infiltration at failure may then be computed. It is also interesting to note the large oscillations in fluid pressure near the ground surface, associated with the non-uniform rainfall time series. These oscillations damp out with depth, however, so that the bedrock interface experiences an essentially monotonic increase in fluid pressure. Also note that it is not necessary to completely saturate the soil before failure occurs.

3. Rainfall model

We model rainfall using a first-order Markov process that has two states: dry and wet. Let $X_t = 0$ when the state is dry, and $X_t = 1$ when it is wet. Markov processes using this two-state model have had some success in modeling rainfall [8, 9, 10]. The first-order model makes the assumption that the probability of the next time period being wet or dry depends only on the current state. In the long term, we have π_0 and π_1 as the probabilities of a state being wet or dry. In [11], a method of choosing the model order is presented, but here we stick with a first-order model for simplicity. We use historical data in order to calibrate a reasonable model. We estimate the transition probabilities of the Markov chain $p_{ij}, i, j = 0, 1$, where p_{ij} is the probability of going from state i at one time step, to state j in the next time step. We then simulate from this Markov model to test the possible effects on slope failure.

During the wet states, the amount of rainfall is modeled as an independent and identically distributed mixed exponential random variable. The mixed exponential model for rainfall amounts has been established as a good fit to some sets of historical rain data [12], and has been used with Markov models [13, 14]. Use of a mixed exponential model suggests that rainfall amounts can be derived from two exponential distributions with different means. The density function is given by

$$f(x) = \frac{\alpha}{\lambda_1} e^{-x/\lambda_1} + \frac{1-\alpha}{\lambda_2} e^{-x/\lambda_2} \tag{6}$$

where α is the parameter that is the proportion of weight given to the first exponential random variable with mean λ_1. We use maximum-likelihood estimation to choose parameters α, λ_1, and λ_2.

As noted in [14], first-order Markov models tend to underestimate the occurrence of long dry spells. In addition to using the Markov parameters fit using maximum likelihood estimation, we simulated rainfall series from Markov chains that have the same long term state probabilities π_0 and π_1, but have different transition probabilities to encourage longer dry periods (and subsequently longer rainy periods). The expected daily rainfall for the models remains unchanged as we still use the same mixed exponential distribution and the same proportion of wet and dry days. However, the rainfall is now distributed differently by having longer rainfall periods, and longer times between rainfalls. This way, we are able to test the slope's resistance to longer wet periods. Fixing π_0 and π_1, we derive the following relationship between p_{00} and p_{11}:

$$p_{00} = \frac{\pi_0 - \pi_1(1 - p_{11})}{\pi_0}, \tag{7}$$

where p_{00} is $P(X_{t+1} = 0|X_t = 0)$, and p_{11} is $P(X_{t+1} = 1|X_t = 1)$. In order for the transition probabilities to be between 0 and 1, we require $1 - \pi_0/\pi_1 \leq p_{11} \leq 1$ and $1 - \pi_1/\pi_0 \leq p_{00} \leq 1$. We simulate rainfall series using different values of p_{00} and p_{11}, where larger values imply longer expected wet or dry periods.

The mean of a mixed exponential random variable is $\alpha\lambda_1 + (1-\alpha)\lambda_2$. The expected rainfall for a given time period is $\mu = \pi_1 (\alpha\lambda_1 + (1-\alpha)\lambda_2)$, because we have π_1 as the long term proportion of days with rainfall. We also run the slope analysis using μ as a constant rainfall rate to compare the results with the simulated time series rainfall results.

4. Results

In order to test the sensitivity of the slope failure model to rainfall patterns, we simulated multiple replications of three stochastic rainfall models. The first model (Set 1) was the the maximum likelihood estimation best fit model, where the Markov parameters were fit from a recorded data history, and the mixed exponential model was fit from the rainfall amounts during wet time periods. The first plot of Figure 3 shows a sample realization of this model. As noted in the literature, simulating from a first-order Markov model tends to produce a more sporadic rainfall pattern than what has been observed historically because the dependence across multiple time steps is not captured. In light of this fact, we also created two additional sets of Markov transition probabilities that would increase the expected length of wet and dry periods. These two models (Sets 2 and 3) have the same long term probabilities π_0 and π_1, but have different transition probabilities p_{00} and p_{11}. The second and third plots of Figure 3 show sample realizations of these models.

The Markov parameters for the three models are provided in Table 2. We also test the slope failure model using uniform rainfall (at the mean value μ derived from the model). Because π_1 remains fixed for the three models we tested, we can compare all three to the constant rainfall model using μ. Each stochastic model was run 100 times, and Table 2 shows the sample mean and standard deviation of the time to failure and total infiltration data collected for each model. The models with the longer expected dry/wet periods have a slightly longer average time to failure, and a much higher variance. This increase in variance may be readily explained from the properties of the Markov chain. For the long wet/dry period models, failure can either happen very early if the rain starts and does not stop for a while, or it can happen much later because the simulation starts in a dry period which lasts a long time.

Figure 4 shows a scatter plot of the time to failure versus the average rainfall rain rate up until failure for the three simulated rainfall models. The red dot on each plot shows the results for the constant rainfall model. By assuming that the total infiltration required to trigger failure, Q, is approximately constant, one may estimate an average rainfall-rate/time-to-failure relationship as

$$q = \frac{Q}{t} \tag{8}$$

This relationship, using the total infiltration Q for the uniform rainfall case, is also plotted in the figure. We see that while the data from a single deterministic simulation may give a reasonable estimate of the rainfall-rate/time-to-failure trend, a single simulation lacks any information on the potential variability resulting from stochastic rainfall

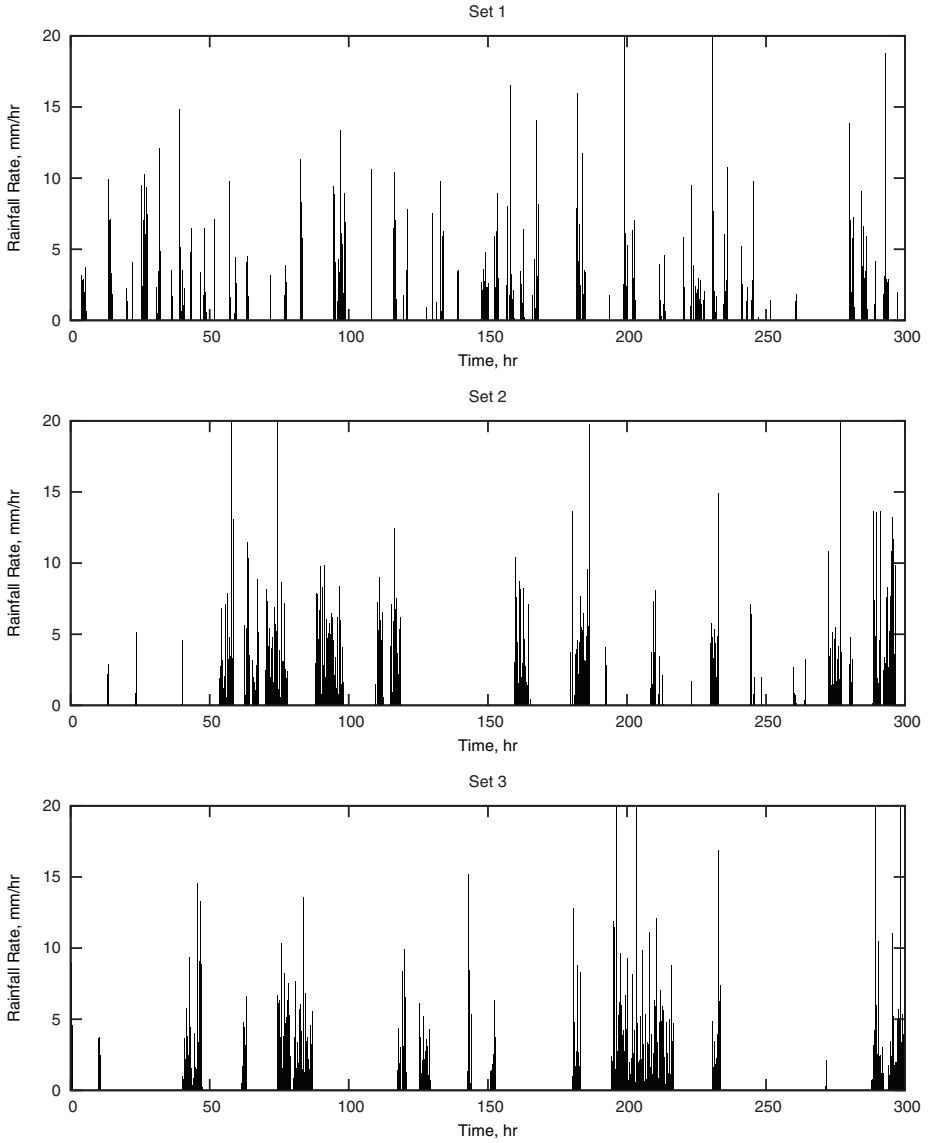

Figure 3: Typical realizations of the rainfall record for each of the three parameter sets.

Table 2: Summary of simulation results.

Experiment	Markov Param.		Time to Failure, hr		Total Infiltration, mm	
	p_{00}	p_{11}	Mean	Std. Dev.	Mean	Std. Dev.
Uniform Rain	–	–	88.08	–	57.18	–
Set 1 (Best Fit)	0.95	0.78	93.75	22.49	58.60	4.90
Set 2	0.98	0.90	98.61	27.02	59.10	6.33
Set 3	0.99	0.97	108.91	60.08	62.60	10.19

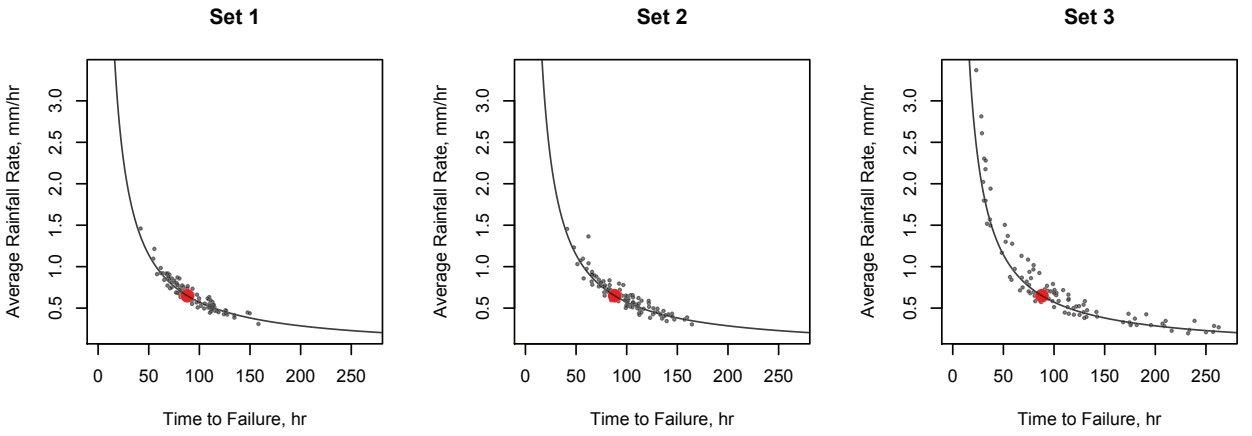

Figure 4: Scatter plot of stochastic simulation results (black dots), and mean rainfall simulation result (red dot). Black line indicates the expected rainfall-rate/time-to-failure relationship inferred from the mean rainfall simulation.

records. Furthermore, we see that this trend line is not strictly conservative, and may overestimate the necessary rainfall required to trigger failure. This is particularly true as the length of dry/wet spells increases.

5. Conclusion

In this work, we have described a Markov model for simulating rainfall time series given a single historical record. We have then used these simulated series to drive many finite element simulations of subsurface infiltration and slope failure. Results indicate that the use of a single "average" rainfall model may give a reasonable estimate of the total infiltration and timing of slope failure, but such approximations are not necessarily conservative. In contrast, by including the inherent uncertainty in future rainfall within a stochastic hazard analysis, one may better assess variability in the slope failure process. These results are therefore much more informative from a risk assessment and management perspective.

Acknowledgements

Portions of this work were performed under the auspices of the U.S. Department of Energy by Lawrence Livermore National Laboratory under Contract DE-AC52-07NA27344.

References

[1] B. A. Ebel, K. Loague, J. E. Vanderkwaak, W. E. Dietrich, D. R. Montgomery, R. Torres, S. P. Anderson, Near-surface hydrologic response for a steep, unchanneled catchment near Coos Bay, Oregon: 2. Physics-based simulations, American Journal of Science 307 (4) (2007) 709–748.
[2] R. I. Borja, J. A. White, Continuum deformation and stability analyses of a steep hillside slope under rainfall infiltration, Acta Geotechnica 5 (1) (2010) 1–14.
[3] R. I. Borja, J. A. White, X. Liu, W. Wu, Factor of safety in a partially saturated slope inferred from hydro-mechanical continuum modeling, International Journal for Numerical and Analytical Methods in Geomechanics 36 (2) (2012) 236–248.
[4] Y. Hong, R. Adler, G. Huffman, Evaluation of the potential of NASA multi-satellite precipitation analysis in global landslide hazard assessment, Geophysical Research Letters 33 (22) (2006) 1–5.
[5] N. Lu, J. Godt, Infinite slope stability under steady unsaturated seepage conditions, Water Resources Research 44 (11) (2008) W11404.
[6] M. T. van Genuchten, A closed-form equation for predicting the hydraulic conductivity of unsaturated soils, Soil Science Society of America Journal 44 (5) (1980) 892–898.
[7] J. A. White, R. I. Borja, Block-preconditioned Newton-Krylov solvers for fully coupled flow and geomechanics, Computational Geosciences 15 (4) (2011) 647–659.
[8] N. Kottegoda, L. Natale, E. Raiteri, Some considerations of periodicity and persistence in daily rainfalls, Journal of Hydrology 296 (1-4) (2004) 23–37.
[9] R. Mehrotra, A. Sharma, A semi-parametric model for stochastic generation of multi-site daily rainfall exhibiting low-frequency variability, Journal of Hydrology 335 (1-2) (2007) 180–193.

[10] J. Roldan, D. A. Woolhiser, Stochastic Daily Precipitation Models 1., Water Resources Research 18 (5) (1982) 1451–1459.
[11] J. T. Schoof, S. C. Pryor, On the Proper Order of Markov Chain Model for Daily Precipitation Occurrence in the Contiguous United States, Journal of Applied Meteorology and Climatology 47 (9) (2008) 2477–2486.
[12] Woolhiser D.A., J. Roldan, Stochastic Daily Precipitation Models: 2. A comparison of distribution amounts., Water Resources Research 18 (5) (1982) 1461–1468.
[13] D. Wilks, Multisite generalization of a daily stochastic precipitation generation model, Journal of Hydrology 210 (1-4) (1998) 178–191.
[14] D. Wilks, Interannual variability and extreme-value characteristics of several stochastic daily precipitation models, Agricultural and Forest Meteorology 93 (1999) 153–169.